J Mater Sci (2009) 44:4953–4958
DOI 10.1007/s10853-009-3756-5

Ferroelectric and piezoelectric properties of $[(Bi_{0.98}La_{0.02}Na_{1-x}Li_x)_{0.5}]_{0.94}Ba_{0.06}TiO_3$ lead-free ceramics

Dunmin Lin · K. W. Kwok

Received: 29 March 2009 / Accepted: 15 July 2009 / Published online: 29 July 2009

Abstract Lead-free ceramics $[(Bi_{0.98}La_{0.02}Na_{1-x}Li_x)_{0.5}]_{0.94}Ba_{0.06}TiO_3$ have been prepared by an ordinary sintering technique and their ferroelectric and piezoelectric properties have been studied. The results of X-ray diffraction reveal that Li^+, Ba^{2+}, and La^{3+} diffuse into the $Bi_{0.5}Na_{0.5}TiO_3$ lattices to form a new solid solution with a pure perovskite structure. The partial substitution of Li^+ lowers the coercive field E_c and improves the remanent polarization P_r. Because of the larger P_r and lower E_c, the ceramic with $x = 0.10$ exhibits optimum piezoelectric properties: $d_{33} = 212$ pC/N and $k_P = 36.1\%$. The partial substitution of Li^+ for Na^+ shifts the depolarization temperature T_d toward low temperature. The ceramics exhibit relaxor characteristic, which is probably resulted from the cation disordering in the 12-fold coordination sites. The temperature dependences of the ferroelectric and dielectric properties suggest that the ceramics contain both the polar and non-polar regions near/above T_d, which cause the polarization hysteresis loop become deformed and the ceramics become depolarized.

Introduction

Lead-based piezoelectric ceramics with perovskite structure based on lead zirconate titanate (PZT) and PZT-based multi-component systems are widely used for piezoelectric actuators, sensors, transducers as well as microelectronic devices because of their excellent piezoelectric properties. However, the use of lead-based materials has caused serious lead pollution and environmental problems because of the high toxicity of lead oxide. Therefore, it is necessary to develop environment-friendly lead-free ferroelectric and piezoelectric ceramics.

$Bi_{0.5}Na_{0.5}TiO_3$ (BNT) ceramic is a perovskite-structured ferroelectric with rhombohedral symmetry. Because of its strong ferroelectricity ($P_r = 38$ μC/cm^2) [1], the BNT ceramic has been considered as one of the promising candidates for lead-free ceramics. However, it also has a high coercive field ($E_c = 7.3$ kV/mm) [1], resulting in the difficulty in the poling of the ceramic. Therefore, the pure BNT ceramic usually exhibits relatively weak piezoelectric properties ($d_{33} = 58$ pC/N) [2]. A number of studies have been carried out to improve the poling process and enhance the piezoelectric properties of the ceramics; these include the formation of solid solutions of BNT with other ABO_3-type ferroelectrics or non-ferroelectrics, e.g., BNT–$BaTiO_3$ [1], BNT–$Bi_{0.5}K_{0.5}TiO_3$[3], BNT–$BiAlO_3$[4], BNT–$Bi_{0.5}K_{0.5}TiO_3$–$KNbO_3$ [5], BNT–$KNbO_3$[6], BNT–$SrTiO_3$ [7], BNT–$Bi_{0.5}K_{0.5}TiO_3$–$BaTiO_3$ [8, 9], $[Bi_{0.5}(Na_{0.7}K_{0.25}Li_{0.05})_{0.5}]TiO_3$–$Ba(Ti_{0.95}Zr_{0.05})O_3$ [10], BNT–$K_{0.5}Na_{0.5}NbO_3$ [11], BNT–BNT–$Bi_{0.5}K_{0.5}TiO_3$–$0.03Ki_{0.5}Na_{0.5}NbO_3$ [12], and BNT–$Bi_{0.5}K_{0.5}TiO_3$–$BiFeO_3$ [13], the substitutions of analogous ions for the A-site $(Bi_{0.5}Na_{0.5})^+$ or B-site Ti^{4+} ions, e.g., $(Bi_{1/2}Na_{1/2})Ti_{1-x}(Ni_{1/3}Nb_{2/3})_xO_3$ [14] and $(Bi_{0.5}Na_{0.5})_{0.94}Ba_{0.06}Zr_yTi_{1-y}O_3$ [15], and the doping of metal oxides, e.g., Nd_2O_3-doped 0.82BNT–0.18$Bi_{0.5}K_{0.5}TiO_3$ [16], Ta-doped 0.94BNT–0.06$BaTiO_3$ [17], and CeO_2-doped $Bi_{0.5}Na_{0.44}K_{0.06}TiO_3$ [18]. It has been noted that as a classical BNT-based system, BNT–$BaTiO_3$ (BNT–BT) ceramics have been reported frequently [1, 17, 19, 20]. For BNT–BT ceramics, the optimum piezoelectric

D. Lin (✉)
College of Chemistry and Materials Science, Sichuan Normal University, Chengdu 610066, People's Republic of China
e-mail: ddmd222@yahoo.com.cn

K. W. Kwok
Department of Applied Physics and Materials Research Centre, The Hong Kong Polytechnic University, Kowloon, Hong Kong, People's Republic of China

properties are achieved at 6 mol.% $BaTiO_3$ because of the existence of morphotropic phase boundary (MPB) but the maximum value of piezoelectric coefficient d_{33} (125 pC/N) is not high enough [1]. Our previous work has also shown that the substitution of a small amount of La^{3+} (2–4 mol.%) for Bi^{3+} in the 0.94BNT–0.06$BaTiO_3$ ceramics can effectively enhance the piezoelectric properties [21]. In the present work, a new BNT-based multi-component solid solution, $[(Bi_{0.98}La_{0.02}Na_{1-x}Li_x)_{0.5}]_{0.94}Ba_{0.06}TiO_3$, was developed by the partial substitutions of 2.5–12.5 mol.% Li^+ for Na^+ and 2 mol.% La^{3+} for Bi^{3+} in the A-sites of 0.94BNT–0.06$BaTiO_3$ ceramics and prepared by an ordinary sintering method, and their microstructure, ferroelectric, and piezoelectric properties were investigated.

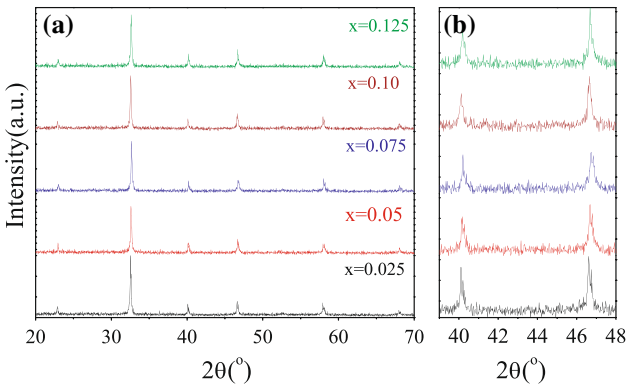

Fig. 1 XRD patterns of the $[(Bi_{0.98}La_{0.02}Na_{1-x}Li_x)_{0.5}]_{0.94}Ba_{0.06}TiO_3$ ceramics

Experimental

$[(Bi_{0.98}La_{0.02}Na_{1-x}Li_x)_{0.5}]_{0.94}Ba_{0.06}TiO_3$ ceramics were prepared by a conventional ceramic fabrication technique using analytical-grade metal oxides or carbonate powders as raw materials: Bi_2O_3 (99%), Na_2CO_3 (99%), Li_2CO_3 (97%), $BaCO_3$ (99%), La_2O_3 (99%), and TiO_2 (99.5%). The powders in the stoichiometric ratio of the compositions were mixed thoroughly in ethanol using zirconia balls for 8 h, and then dried and calcined at 850 °C for 2 h. After the calcination, the mixture was ball milled again for 8 h and mixed thoroughly with a PVA binder solution, and then pressed into disk samples. The disk samples were sintered at 1,100 °C for 2 h in air. For electrical measurements, silver electrodes were fired on the top and bottom surfaces of the samples at 730 °C for 15 min. The samples were poled at room temperature under a dc field of 5–6 kV/mm in a silicon oil bath for 30 min.

The crystalline structure of the sintered samples was examined using X-ray diffraction (XRD) analysis with CuK_α radiation (DX-1000). The microstructure was observed using a scanning electron microscope (JEOL JSM-5900LV). The relative permittivity ε_r and loss tangent tanδ of the ceramics at 1, 10, and 100 kHz were measured as functions of temperature using an impedance analyzer (Agilent 4192A). A conventional Sawyer-Tower circuit was used to measure the polarization hysteresis (P–E) loop at 50 Hz. The planar electromechanical coupling factor k_p and mechanical quality factor Q_m were determined by the resonance method according to the IEEE Standard using an impedance analyzer (Agilent 4294A). The piezoelectric coefficient d_{33} was measured using a piezo-d_{33} meter (ZJ-3A, China).

Results and discussion

The XRD patterns of the $[(Bi_{0.98}La_{0.02}Na_{1-x}Li_x)_{0.5}]_{0.94}Ba_{0.06}TiO_3$ ceramics are shown in Fig. 1. All the ceramics possess a pure perovskite structure, suggesting that Li^+, Ba^{2+}, and La^{3+} have diffused into the BNT lattices to form a new homogeneous solid solution (Fig. 1a). Similar to the 0.94BNT–0.06$BaTiO_3$ ceramic [1], all the $[(Bi_{0.98}La_{0.02}Na_{1-x}Li_x)_{0.5}]_{0.94}Ba_{0.06}TiO_3$ ceramics reside within the MPB. This is evidenced by the splitting of the (003)/(021) characteristic peaks between 39° and 41° and the splitting of the (002)/(200) characteristic peaks between 46° and 48° as observed in the $[(Bi_{0.98}La_{0.02}Na_{1-x}Li_x)_{0.5}]_{0.94}Ba_{0.06}TiO_3$ ceramics (Fig. 1b), indicating that the substitutions of Li^+ for Na^+ and 2 mol.% La^{3+} for Bi^{3+} do not cause any significant change to the crystalline structure.

The SEM micrographs of the $[(Bi_{0.98}La_{0.02}Na_{1-x}Li_x)_{0.5}]_{0.94}Ba_{0.06}TiO_3$ ceramics with $x = 0.05$ and 0.10 are shown in Fig. 2. Both the ceramics are well-sintered at 1,100 °C for 2 h, are dense and pore-free, having a relative density (measured by the Archimedes method) larger than 97%. It can be seen that the substitution of Li is effective in suppressing the grain growth. For the ceramic with $x = 0.05$, the average grain size is about 5.7 μm (Fig. 2a). As x increases to 0.10, the grain size decreases significantly to ~3.0 μm (Fig. 1b). Similar results have been observed for the BNT–$Bi_{0.5}K_{0.5}TiO_3$ ceramics [22], for which the grain size was reduced significantly after the addition of K^+. It has been noted that, as compared to the Li-free BNT-based ceramics, the $[(Bi_{0.98}La_{0.02}Na_{1-x}Li_x)_{0.5}]_{0.94}Ba_{0.06}TiO_3$ ceramics can be well-sintered at a lower temperature (1,100 vs. 1,150–1,250 °C [1–10]). This may be attributed to the formation of the liquid phase arisen from the low melting temperature of the Li-containing compounds.

The P–E loops measured under an electric field of 7 kV/mm at room temperature for the $[(Bi_{0.98}La_{0.02}Na_{1-x}Li_x)_{0.5}]_{0.94}Ba_{0.06}TiO_3$ ceramics with $x = 0.025$, 0.05, 0.10, and 0.125 are shown in Fig. 3a, while the compositional dependences of the remanent polarization P_r and coercive field E_c are shown in Fig. 3b. All the ceramics exhibit a

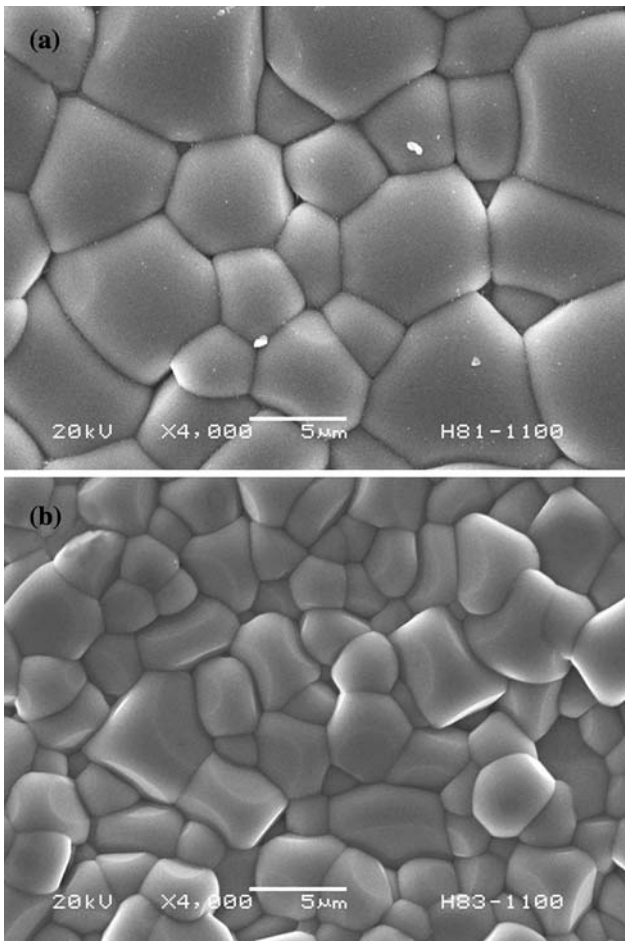

Fig. 2 SEM micrographs of the $[(Bi_{0.98}La_{0.02}Na_{1-x}Li_x)_{0.5}]_{0.94}Ba_{0.06}TiO_3$ ceramics with **a** $x = 0.05$ sintered at 1,100 °C for 2 h; **b** $x = 0.10$ sintered at 1,100 °C for 2 h

typical and saturated *P–E* loop. As shown in Fig. 3a, the ceramic with $x = 0.025$ exhibits well-saturated and square-like *P–E* loops with P_r and E_c of 43.0 μC/cm^2 and 3.90 kV/mm. As x increases from 0.025 to 0.10, the E_c is lowered but simultaneously the P_r is increased. However, as x further increases to 0.125, the *P–E* loop becomes slightly flattened and slanted, giving a much smaller P_r. As shown in Fig. 3b, the observed P_r increases with increasing x and then decreases, giving a maximum value of 47.2 μC/cm^2 at $x = 0.05$, while the observed E_c decreases from 3.90 to 2.76 kV/mm as x increases from 0.025 to 0.125. As compared to the pure BNT ceramic ($P_r = 38$ μC/cm^2 and $E_c = 7.3$ kV/mm), the present ceramics possess the much larger P_r and lower E_c. The large remanent polarization favors the piezoelectricity, while the low coercive field should facilitate the poling process.

The variations of d_{33}, k_p, Q_m, ε_r, and tanδ with x for the $[(Bi_{0.98}La_{0.02}Na_{1-x}Li_x)_{0.5}]_{0.94}Ba_{0.06}TiO_3$ ceramics are shown in Fig. 4. As shown in Fig. 4a, the observed d_{33} increases with increasing x and then decreases, giving the

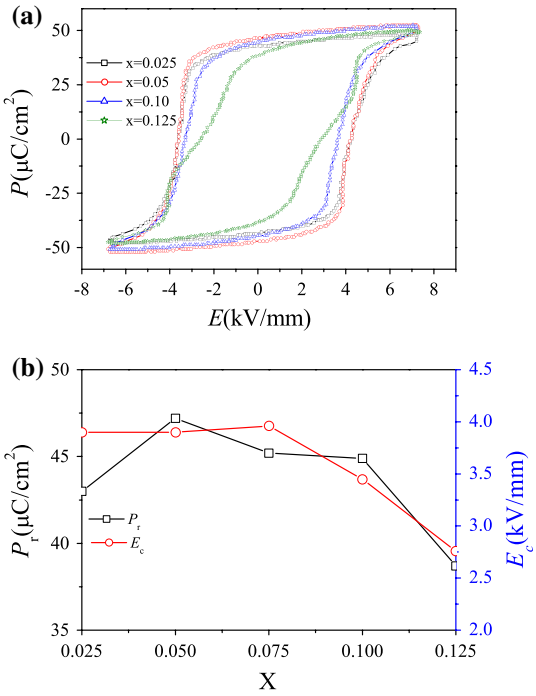

Fig. 3 **a** *P–E* loops for the $[(Bi_{0.98}La_{0.02}Na_{1-x}Li_x)_{0.5}]_{0.94}Ba_{0.06}TiO_3$ ceramics with $x = 0.025$, 0.05, 0.10, and 0.125 at room temperature; **b** Variations of P_r and E_c of the $[(Bi_{0.98}La_{0.02}Na_{1-x}Li_x)_{0.5}]_{0.94}Ba_{0.06}TiO_3$ ceramics with x

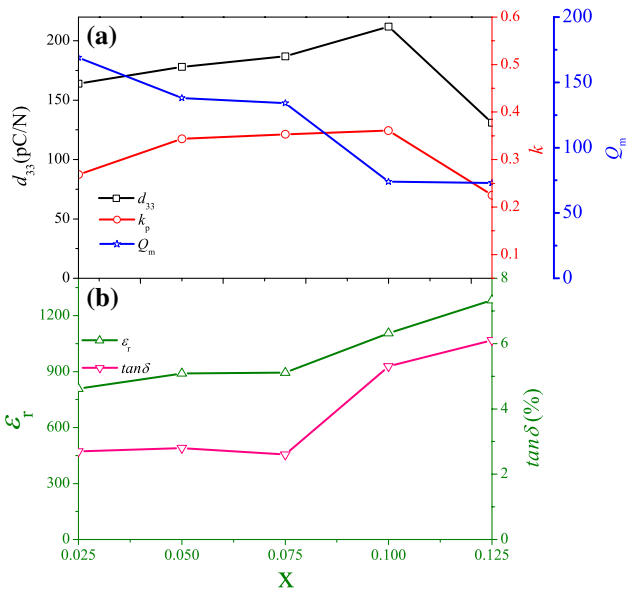

Fig. 4 Compositional dependences of d_{33}, k_p, Q_m, ε_r, and tanδ for the $[(Bi_{0.98}La_{0.02}Na_{1-x}Li_x)_{0.5}]_{0.94}Ba_{0.06}TiO_3$ ceramics

maximum values of 212 pC/N at $x = 0.10$. The observed k_p exhibits a similar variation with x and has an optimum value of 36.1% at $x = 0.10$ (Fig. 4a). From Fig. 4b, at $x \leq 0.075$, the observed ε_r and tanδ have weak dependences on x but when $x > 0.075$, the ε_r and tanδ increase

greatly with x. It can be seen that the observed Q_m decreases significantly as x increases (Fig. 4a). This suggests that after the substitution of Li^+ for Na^+, the ceramics become "softened", thus giving rise to significant improvements in d_{33}, k_p, and ε_r. As compared to the pure BNT and classic 0.94BNT–$BaTiO_3$ ceramics, the present ceramics exhibits much better piezoelectric properties. The significant improvements in piezoelectric properties of the $[(Bi_{0.98}La_{0.02}Na_{1-x}Li_x)_{0.5}]_{0.94}Ba_{0.06}TiO_3$ ceramics should also be attributed to the lower E_c, larger P_r and the existence of MPB. According to the phenomenological theory, d_{33} is related to ε_r, the spontaneous polarization P_s (which may be approximated by P_r) and the electrostrictive coefficient Q_{11} via a general equation $d_{33} = 2Q_{11}\varepsilon_0\varepsilon_r P_s$ [23]. As shown in Figs. 3 and 4, the ceramic with $x = 0.10$ possesses a relative large P_r (44.9 μC/cm^2) and a relatively high ε_r (1106), and so it exhibits the largest d_{33}.

Figure 5 shows the temperature dependences of ε_r and tanδ at 1, 10, and 100 kHz for the poled $[(Bi_{0.98}La_{0.02}Na_{1-x}Li_x)_{0.5}]_{0.94}Ba_{0.06}TiO_3$ ceramics with $x = 0.025$, 0.05, 0.075, and 0.10. Similar to the other BNT-based ceramics [1–10], all the $[(Bi_{0.98}La_{0.02}Na_{1-x}Li_x)_{0.5}]_{0.94}Ba_{0.06}TiO_3$ ceramics exhibit two dielectric anomalies at T_d and T_m. T_d is the depolarization temperature which corresponds to a transition from a ferroelectric state to a so-called "anti-ferroelectric" state, while T_m is the maximum temperature at which ε_r reaches a maximum value. T_d can also be derived from the peak in the temperature plot of tanδ [3]. As shown in Fig. 5a–d, the observed T_d for the $[(Bi_{0.98}La_{0.02}Na_{1-x}Li_x)_{0.5}]_{0.94}Ba_{0.06}TiO_3$ ceramics decreases from 91 to 58 °C and T_m decreases from 252 to 185 °C as x increase from 0.025 to 0.10. From Fig. 5, it is also seen that for all the ceramics, ε_r exhibits a strong frequency dependence at T_m, and the maximum value of ε_r decreases as frequency increases while the corresponding T_m increases, suggesting that the $[(Bi_{0.98}La_{0.02}Na_{1-x}Li_x)_{0.5}]_{0.94}Ba_{0.06}TiO_3$ ceramics are relaxor ferroelectrics and the phase transition at T_m is a diffuse phase transition. Diffuse phase transition has been observed in many ABO_3-type perovskites and bismuth layer-structured compounds, such as BNT-based ceramics [9], $K_{0.5}La_{0.5}Bi_2Nb_2O_9$ [24], $Pb(Mg_{1/3}Nb_{2/3})O_3$ [25], of which either the A-sites or B-sites are occupied by at least two cations. For the $[(Bi_{0.98}La_{0.02}Na_{1-x}Li_x)_{0.5}]_{0.94}Ba_{0.06}TiO_3$ ceramics, Na^+, Bi^{3+}, Li^+, La^{3+}, and Ba^{2+} are randomly distributed in the 12-fold coordination sites, so the observed diffuse phase transition behavior at T_m is reasonably attributed to the disordering of A-site cations and the local compositional fluctuation.

The variations of the P–E loops with temperature for $[(Bi_{0.98}La_{0.02}Na_{1-x}Li_x)_{0.5}]_{0.94}Ba_{0.06}TiO_3$ ceramics with $x = 0.05$ and 0.10 are shown in Fig. 6. Both the ceramics exhibit a typical ferroelectric P–E loop at room temperature. For the ceramic with $x = 0.05$, as temperature increases to 60 °C, E_c decreases and hence the loop becomes more saturated, giving a large P_r value of 45.1 μC/cm^2. However, as temperature increases to 70 °C, the loop becomes slightly deformed but the large P_r is maintained ($P_r = 42.7$ μC/cm^2). When temperature further increases to 80 °C, the P–E loop become flatted, slanted and deformed and is different from the typical ferroelectric characteristics, and P_r decreases quickly to 16.5 μC/cm^2. At higher temperature, the P–E loop becomes slanted, narrow and slim gradually. At 160 °C, the loop becomes very slim and narrow, giving a very small value of P_r

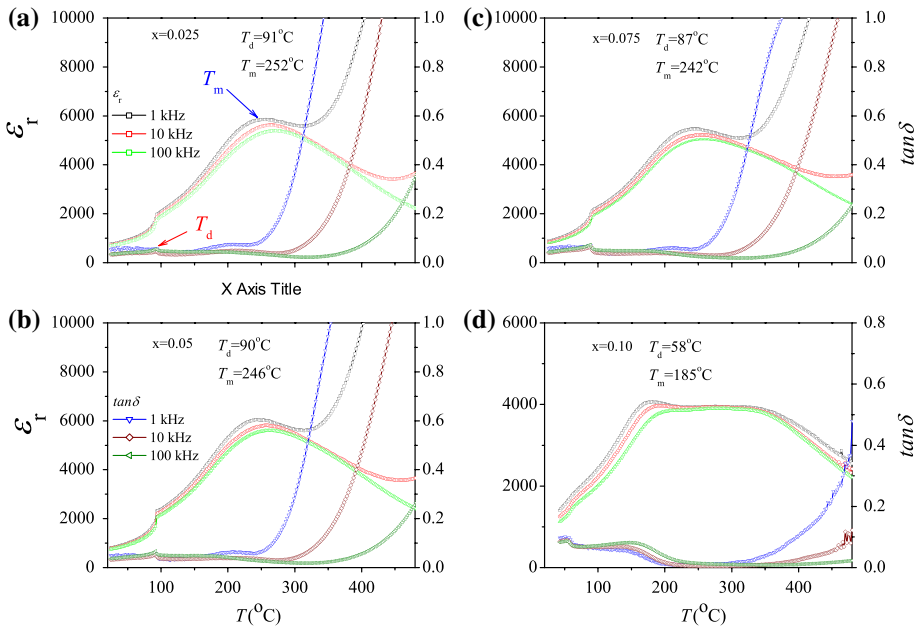

Fig. 5 Variations of ε_r and tanδ with temperature for the $[(Bi_{0.98}La_{0.02}Na_{1-x}Li_x)_{0.5}]_{0.94}Ba_{0.06}TiO_3$ ceramics at 1, 10, and 100 kHZ: **a** $x = 0.025$; **b** $x = 0.05$; **c** $x = 0.075$; and **d** $x = 0.10$

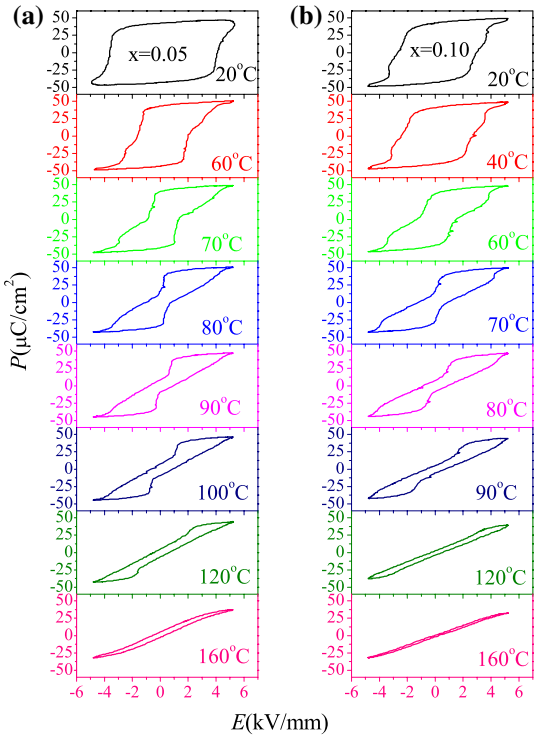

Fig. 6 *P–E* loops of the $[(Bi_{0.98}La_{0.02}Na_{1-x}Li_x)_{0.5}]_{0.94}Ba_{0.06}TiO_3$ ceramics at different temperatures: **a** $x = 0.025$; **b** $x = 0.10$

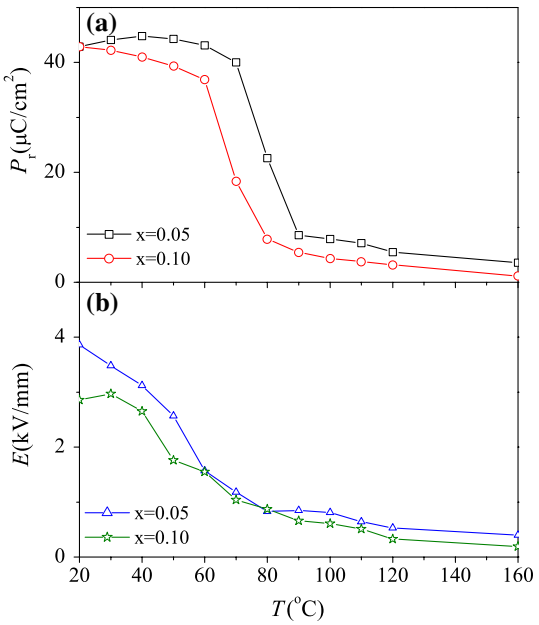

Fig. 7 Variations of P_r and E_c with temperature for the $[(Bi_{0.98}La_{0.02}Na_{1-x}Li_x)_{0.5}]_{0.94}Ba_{0.06}TiO_3$ ceramics with $x = 0.05$ and 0.10

(4.89 μC/cm^2). As determined from Fig. 6a, the depolarization temperature T_d of the ceramic with $x = 0.05$ is about 80–90 °C, which is close to the value determined from the temperature plot of tanδ (91 °C) (Fig. 5b). From Fig. 6b, the ceramic with $x = 0.10$ exhibits similar temperature dependence of the ferroelectric properties, and possesses a well-saturated *P–E* loop below T_d and a slightly deformed one above T_d, revealing a T_d value of about 60–70 °C. Although the loops at high temperatures ($>T_d$, especially 160 °C) are very slim, they are still similar to a ferroelectric hysteresis loop, and are clearly not a double-loop of antiferroelectric ceramics [26]. Besides, the forward switching field ($E_{AFE\text{-}FE}$), at which the antiferroelectric domains align to become ferroelectric domains [27], cannot be observed in the loops (Fig. 6). Recently, it has been shown that, by in situ transmission electron microscopy (TEM), there is no crystallographic evidence of antiferroelectric domains near T_d [15, 27] and the depolarization is induced by the weakening of the macroscopic ferroelectric domains [27]. Together with the temperature dependence of ferroelectric and dielectric properties (Figs. 5, 6), it has been suggested that the anomalies in *P–E* loop were resulted from the electro-mechanical interaction between the polar and non-polar regions which coexisted in the BNT-based ceramics near T_d [6, 7, 15, 28]. Therefore, on the basis of the above results, it is suggested that the polar region and non-polar region may coexist in the $[(Bi_{0.98}La_{0.02}Na_{1-x}Li_x)_{0.5}]_{0.94}Ba_{0.06}TiO_3$ ceramics near/above T_d and their interaction causes the *P–E* loops become deformed at high temperatures near/above T_d.

The temperature dependences of P_r and E_c for the $[(Bi_{0.98}La_{0.02}Na_{1-x}Li_x)_{0.5}]_{0.94}Ba_{0.06}TiO_3$ ceramics with $x = 0.05$ and 0.10 are shown in Fig. 7. From Fig. 7, P_r has the large values and keeps almost unchangeable at temperature below T_d. However, as temperature increases above T_d, P_r decreases greatly, showing clearly the ferroelectric—"non-ferroelectric" phase transition. Different from P_r, E_c decreases with increasing temperature.

Conclusions

A new Li-modified BNT-based lead-free solid solution, $[(Bi_{0.98}La_{0.02}Na_{1-x}Li_x)_{0.5}]_{0.94}Ba_{0.06}TiO_3$, has been developed and prepared by an ordinary sintering technique. The results of X-ray diffraction reveal that the ceramics possess a pure perovskite structure. All the ceramics can be well-sintered at a relatively low sintering temperature (1,100°C). After the substitution of Li^+ for Na^+, the ceramics exhibit a lower E_c, a larger P_r and thus improved piezoelectric properties. For the ceramic with $x = 0.10$, the piezoelectric properties become optimum, giving $d_{33} = 212$ pC/N and $k_P = 36.1\%$. The ceramics also exhibit deformed or slim *P–E* loops at high temperatures near/above T_d, suggesting that the ceramics may contain both the polar and non-polar regions near/above T_d.

Acknowledgement This work was supported by the Projects of Education Department of Sichuan Province (08ZA047), and Science and Technology Bureau of Sichuan Province (09ZQ026-059).

References

1. Takennaka T, Maruyama K, Sakata K (1991) Jpn J Appl Phys 30:2236
2. Herabut A, Safari A (1997) J Am Soc 80:2954
3. Yoshii K, Hiruma Y, Nagata H, Takenaka T (2006) Jpn J Appl Phys 45:4493
4. Yu H, Ye ZG (2008) Appl Phys Lett 93:112902
5. Fan G, Lu W, Wang X, Liang F (2007) Appl Phys Lett 91:202908
6. Fan G, Lu W, Wang X, Liang F, Xiao J (2008) J Phys D: Appl Phys 41:035403
7. Hiruma Y, Imai Y, Watanabe Y, Nagata H, Takenaka T (2008) Appl Phys Lett 92:262904
8. Zhang S, Shrout TR, Nagata H, Hiruma Y, Takenaka T (2007) IEEE Trans Ultrason Ferroelect Freq Contr 54:910
9. Li Y, Chen W, Xu Q, Zhou J, Gu X, Fang S (2005) Mater Chem Phys 94:328
10. Zhang Z, Jia J, Yang H, Chen C, Sun H, Hu X, Yang D (2008) J Mater Sci 43:1501. doi:10.1007/s10853-007-2382-3
11. Kounga AB, Zhang ST, Jo W, Granzow T, Rödel J (2008) Appl Phys Lett 92:222902
12. Yao Z, Liu H, Chan L, Cao M (2009) Mater Lett 65:547
13. Zhou C, Liu X, Li W, Yuan C (2009) Mater Chem Phys 114:832
14. Zhou CR, Liu XY (2008) J Alloys Compd 466:563
15. Yao YQ, Tseng TY, Chou CC, Chen HHD (2007) J Appl Phys 102:094102
16. Yang Z, Hou Y, Liu B, Wei L (2008) Ceram Int. doi: 10.1016/j.ceramint.2008.07.014
17. Zuo R, Ye C, Fang X, Li J (2008) J Eur Ceram Soc 28:871
18. Li Y, Chen W, Xu Q, Zhou J, Wang Y, Sun H (2007) Cerarm Int 33:95
19. Chu BJ, Chen DR, Li GR, Yin QR (2002) J Eur Ceram Soc 22:2115
20. Zhou XY, Gu HS, Wang Y, Li WY, Zhou TS (2005) Mater Lett 59:1649
21. Zheng Q, Xu C, Lin D, Gao D, Kwok KW (2008) J Phys D: Appl Phys 41:125411
22. Zhao S, Li G, Ding A, Wang T, Yin Q (2006) J Phys D: Appl Phys 39:2277
23. Damjanovic D (1998) Rep Prog Phys 61:1267
24. Karthik C, Ravishankar N, Varma KBR (2006) Appl Phys Lett 89:1760
25. Uchino K, Nomura S, Cross LE, Tang SJ, Newnham RE (1980) J Appl Phys 15:1142
26. Haertiling GH (1999) J Am Ceram Soc 82:797
27. Tai CWT, Choy SH, Chan HLW (2008) J Am Ceram Soc 91:3335
28. Suchanicz J, Kusz J, Böhm H, Duda H, Mercurio JP (2003) J Eur Ceram Soc 22:1559